scientific reports

OPEN

Clinicopathological features and mucin expression of early papillary gastric adenocarcinoma

Jiaqi Chen[1], Xiujie Cui[2], Chengjun Zhou[2✉] & Mulan Jin[1✉]

Early papillary gastric adenocarcinoma (EPGA), a well-differentiated gastric adenocarcinoma, is characterized by higher malignancy and worse prognosis compared to other differentiated gastric adenocarcinomas. Therefore, there is a critical need to elucidate its clinicopathological features and mucin expression for accurate diagnosis. The data of 116 cases of EPGA and 116 cases of early well-moderately differentiated tubular gastric adenocarcinoma (ETGA) diagnosed via pathological examination following radical gastrectomy from January 2016 to December 2023 at the Second Hospital of Shandong University were collected. Multivariable logistic regression was used to conduct a comparative analysis of the two groups of variables. The features of histological grading and immunophenotype, particularly mucin expression, were specifically analyzed. The receiver operating characteristic (ROC) curve analysis was used to assess the diagnostic efficacy of potential biomarkers in distinguishing EPGA from ETGA. The features of histological grading and MUC5AC expression in EPGA were specifically analyzed. Additionally, the risk factors of LVI in early gastric cancer (EGC) were assessed. EPGA exhibited significantly larger size ($P < 0.001$), higher frequencies of elevated appearance ($P = 0.001$), ulcer formation ($P = 0.010$) and lymphovascular invasion (LVI, $P = 0.050$) compared to ETGA. The expression of mismatch repair-deficient ($P = 0.005$) and MUC5AC ($P < 0.001$) were significantly elevated in EPGA compared to ETGA. Compared to ETGA, high-grade EPGA exhibited a greater incidence of ulcer formation ($P < 0.001$), submucosal invasion ($P = 0.007$), LVI ($P = 0.010$) and microsatellite instability-high (MSI-H, $P < 0.001$), whereas low-grade EPGA demonstrated clinicopathological characteristics similar to ETGA. MUC5AC expression was associated with LVI ($P = 0.034$) and MUC6 ($P = 0.017$) in EPGA. Moreover, high expression of MUC5AC showed good diagnostic efficiency in distinguishing EPGA (AUC = 0.724, 95% CI = 0.66–0.79). When EGC infiltrated the submucosa (OR = 25.227, 95% CI = 4.017–158.432; $P < 0.001$) or exhibited MSI-H phenotypes (OR = 10.708, 95% CI = 1.478–77.565; $P = 0.019$), LVI was more likely to occur. The retrospective study elucidates the clinicopathological features and mucin expression profiles of EPGA. The complex architecture and pronounced nuclear atypia observed in high-grade EPGA are indicative of higher malignancy. Moreover, the high expression of MUC5AC suggests a strong likelihood of EPGA, which may aid in its differentiation. In addition, MSI correlates with the presence of LVI in EGC.

Keywords Early papillary gastric adenocarcinoma, Clinicopathological features, Mucins, MUC5AC, Microsatellite instability

Gastric cancer (GC) is the fifth most common malignancy worldwide and the fourth leading cause of cancer-related deaths[1]. Gastric adenocarcinoma is the predominant histological subtype of GC[2]. According to the World Health Organization (WHO) classification[3], GC is categorized into five primary histological types: tubular, papillary, mucinous, poorly cohesive, and mixed carcinomas. Among these, tubular gastric adenocarcinoma (TGA) is the most prevalent, while papillary gastric adenocarcinoma (PGA) is relatively rare. In the Japanese classification of gastric carcinoma, both PGA and well-moderately differentiated TGA are categorized as differentiated types[4].

Early gastric cancer (EGC) is defined as cancer confined to the mucosal or submucosal layers, regardless of lymph node metastasis (LNM)[5]. Early papillary gastric adenocarcinoma (EPGA), an uncommon subtype of EGC, usually contains tubular components with papillary carcinoma glands[6]. Histologically, EPGA is

[1]Department of Pathology, Beijing Chaoyang Hospital of Capital Medical University, Beijing, China. [2]Department of Pathology, The Second Hospital of Shandong University, Jinan, Shandong Province, China. ✉email: chengjunzhou@126.com; kinmokuran@163.com

predominantly well-differentiated, characterized by elongated, finger-like processes lined with columnar or cuboidal cells, supported by fibrovascular connective tissue cores[3]. EGC with well-differentiated histology is generally associated with a more favorable prognosis[7]. However, several studies have indicated that EPGA exhibits a higher malignant potential, evidenced by an increased propensity for deep invasion, lymphovascular invasion (LVI), and LNM[8–10]. Compared to early tubular gastric adenocarcinoma (ETGA), EPGA is more frequently linked with poorly differentiated adenocarcinoma components[11]. Furthermore, Cheng et al. reported that patients with high-grade EPGA exhibit a poorer prognosis than those with ETGA[12]. Although numerous studies have investigated the clinicopathological and molecular characteristics of EPGA[13–17], the majority have focused on microsatellite instability (MSI) and the risk factors influencing the prognosis of EPGA. Insights into the mucin expression for diagnosing EPGA remain limited (Fig. 1).

Mucin, which are high-molecular-weight glycoproteins found in gastric mucus, serve a protective function for the gastric mucosa and are typically expressed in non-neoplastic gastric tissue[18–20]. In normal gastric mucosa, MUC2 is not expressed. MUC5AC is localized within the cytoplasm of gastric foveolar epithelial cells and neck mucous cells, whereas MUC6 is present in the cytoplasm of the gastric pyloric glands, as well as in the neck mucous cells and chief cells of the gastric body[21,22]. Alterations in mucin expression levels are closely linked to gastric preneoplastic lesions and GCs[23]. Since the year 2000, the gastric and intestinal phenotypes of GC have been examined through immunohistochemical analysis, employing MUC5AC and MUC6 as markers for the gastric phenotype, and MUC2 and CD10 (or villin) as markers for the intestinal phenotype. Based on the expression of these markers, GC cases are classified into four phenotypes: gastric or foveolar (G-type), intestinal (I-type), gastric and intestinal mixed (GI-type), and neither gastric nor intestinal (N-type)[24–26]. Koseki K et al. have reported that PGA or mixed tumors with papillary components are more frequently observed in G-type GC, characterized by the expression of MUC5AC and MUC6[27]. Consistent with this study, our routine observations have anecdotally noted that certain cases of EPGA exhibit significantly elevated levels of MUC5AC expression compared to other differentiated gastric adenocarcinomas. However, these emerging insights into EPGA have not been thoroughly investigated.

Therefore, the present study aims to elucidate the clinicopathological features and mucin expression profiles of EPGA. The objective is to deepen the comprehension of these tumors among pathologists and clinicians and to identify potential markers for the diagnosis and differential diagnosis of EPGA.

Methods

Patients and specimens

The clinical data of patients who underwent radical gastrectomy at the Second Hospital of Shandong University between January 2016 and December 2023, with pathological confirmation of EPGA, were collected. Cases of early well-moderately differentiated tubular gastric adenocarcinoma (ETGA) served as the control group. The inclusion criteria for cases were as follows: (1) patients who underwent radical gastrectomy; (2) diagnosis confirmed by postoperative pathological results in accordance with the 5 th WHO Classification of Tumors of
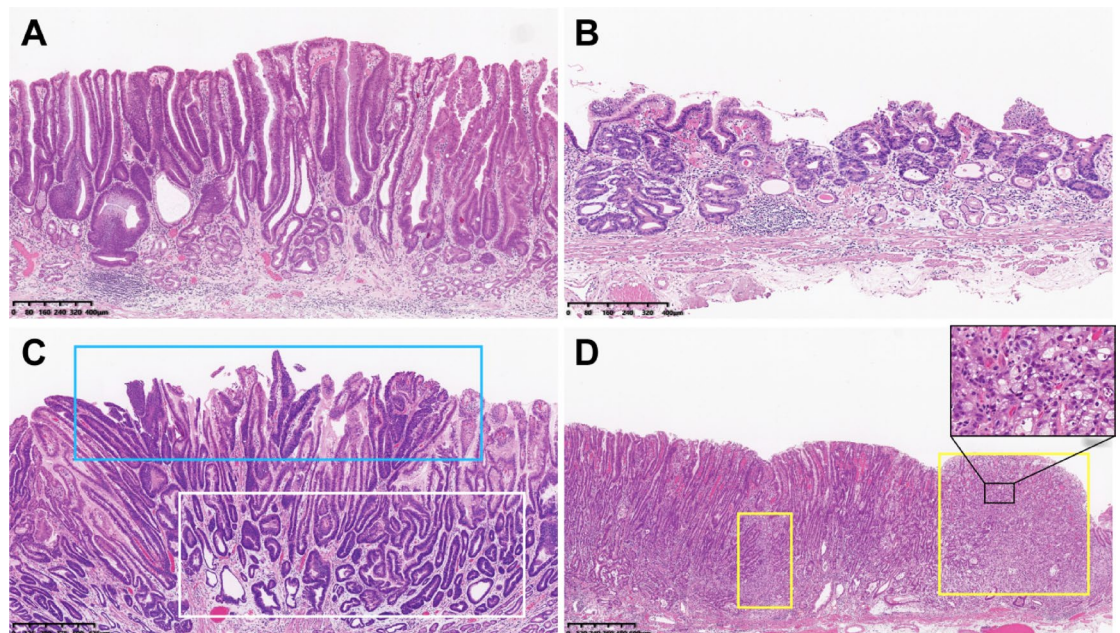

Fig. 1. The histopathologic characteristics of EPGA and ETGA. (A) EPGA is characterized by well-differentiated papillary structures with a central fibrovascular core. (B) ETGA consists of dilated or slit-like branching tubules. (C) Cases of EPGA contain both papillary adenocarcinoma (blue frame) and tubular adenocarcinoma (white frame) components. (D) Cases of EPGA are characterized by poorly differentiated carcinoma components (yellow frames), with signet ring cell carcinoma observable in the magnified image.

the Digestive System (2019 version), identifying either papillary gastric adenocarcinoma or well-moderately differentiated tubular gastric adenocarcinoma; and (3) tumors confined to the mucosa (T1a) or submucosa (T1b), regardless of the presence of lymph node metastasis (LNM). The exclusion criteria included: (1) incomplete pathological data; (2) ambiguous pathological diagnoses; (3) cases with multiple synchronous gastric cancers, local recurrences, or cancers in the remnant stomach or gastric tube; (4) cases that received neoadjuvant chemotherapy or endoscopic operation before surgery; and (5) EPGA cases with papillary components less than 50%. Finally, a total of 232 cases were selected for this research, comprising 116 cases of EPGA and 116 cases of ETGA, with the clinical criteria for surgical intervention being consistent across all cases.

The study protocol received approval from the Medical Ethics Committee of the Second Hospital of Shandong University (KYLL2025373). Informed consent was obtained from all participants which were involved in the study. All procedures involving human participants adhered to the ethical standards of both the institutional and national research committees, as well as the Declaration of Helsinki.

Clinicopathological parameters

Anatomically, the stomach was divided into four regions: (1) the cardia, (2) the fundus, (3) the corpus, and (4) the pylorus[28]. The gross appearance of the tumors was classified into five patterns based on the Paris classification[29]: (1) broad-based protruding (type I), (2) slightly elevated-rough (type IIa), (3) flat (type IIb), (4) superficially depressed (type IIc), and (5) excavated ulcer (type III). In this study, tumors were categorized into two groups: types I and IIa were classified as elevated, while the remaining types were classified as non-elevated[30]. The depth of tumor penetration was assessed microscopically and classified into two subgroups: (1) mucosa (M), where the tumor infiltrates the lamina propria or muscularis mucosae, and (2) submucosa (SM), where the tumor invades the submucosa. Additionally, lymphovascular invasion (LVI) and LNM were included in the analysis[31]. The pattern of tumor infiltration (INF) was categorized in accordance with the 3rd edition of the Japanese Classification of Gastric Cancer[31], leading to the classification of tumors into three groups: (1) INFa, characterized by tumor expansion with a distinct margin separating it from the surrounding tissue; (2) INFc, where the tumor infiltrates without a distinct margin; and (3) INFb, representing an intermediate pattern between INFa and INFc[32]. Ulcer formation was defined as a deformation of the muscularis mucosa or fibrosis evident in the SM layer[33].

EPGA is defined as a tumor in which more than 50% of the tumor area contained papillary structures, as confirmed by three pathologists[33]. Histologically, EPGA is characterized by the presence of early gastric adenocarcinoma with papillary epithelium, distinguished by a central fibrovascular core. In contrast, ETGA is defined by dilated or slit-like branching tubules[34]. The histological features of high-grade EPGA are determined by the extent of nuclear atypia and architectural complexity, which include: (1) complex growth patterns resembling papillary or serrated surfaces, tufting, and slits; and (2) the presence of floating single cells or small clusters of malignant cells on the mucosal surface or within gland lumens, sometimes accompanied by intraluminal necrosis. The nuclei are observed notably enlarged, pleomorphic, and hyperchromatic, with prominent nucleoli. Occasionally, neoplastic cells exhibit oxyphilic or transparent cytoplasm, extending into the glandular lumen in a hobnail-like manner. Furthermore, a high mitotic rate, exceeding 10 per 10 high-power fields (HPF), is observed. EPGA is classified as high-grade if it fulfills at least three of these criteria in more than 20% of the papillary component; otherwise, it is classified as low-grade (Fig. 2). In accordance with the methodology outlined by Nakashima et al.[35], EPGA was further stratified into high-nuclear and low-nuclear grade groups for comprehensive analysis, based on the degree of nuclear polymorphism and polarity.

Immunohistochemical parameters

All paraffin-embedded EPGA and ETGA specimens were sectioned into 4 mm slices and subjected to hematoxylin and eosin (HE) staining as well as immunohistochemical (IHC) staining. Antibodies for biomarkers, including MUC2, MUC5AC, MUC6, MLH1, MSH2, MSH6, PMS2, P53, and Ki-67, were procured from Beijing Zhongshan Golden Bridge Biotechnology Co., Ltd. The IHC results were collaboratively reviewed and quantified by three experienced pathologists using a multi-headed microscope. The expression levels of mucin (MUC2, MUC5AC, and MUC6) in tumor cells were evaluated using the IHC score calculated by multiplying the intensity score and extent score. The intensity score was graded by staining in the cytoplasm of positive tumor cells (no staining = 0; weak staining = 1; moderate staining = 2; strong staining = 3), while the extent score was defined as the percentage of stained cytoplasm (0–100%). Three distinct visual fields (×20 magnification) were selected from each slice to assess the percentage of positive tumor cells (0%=0; 1–25%=1; 26–50%=2; 51–75%=3; >75%=4). The final score, ranging from 0 to 12, was calculated by multiplying the extent score (0–4) by the intensity score (0–3)[36] and classified into low expression (final score < 6) and high expression (final score ≥ 6)[18]. The status of microsatellite instability (MSI) was assessed by analyzing the expression of mismatch repair (MMR) proteins within tumor cells[37]. MMR protein expression, including MLH1, MSH2, MSH6, and PMS2, was classified as mismatch repair-deficient (dMMR) if at least one protein was absent, or mismatch repair-proficient (pMMR) if all proteins were present[38]. Typically, dMMR and pMMR are indicative of the microsatellite instability-high (MSI-H) phenotype and the microsatellite instability-low/microsatellite stable (MSI-L/MSS) phenotype, respectively[39]. The expression of P53 was assessed and categorized as either wild type (negative) or mutant type (positive)[40]. Ki-67 expression was quantified as the average percentage of tumor cells exhibiting strong and diffuse nuclear staining across 10 HPF[30].

Statistical analysis

Statistical analyses were conducted using SPSS version 27.0 (SPSS Inc.). The Student's t-test was employed to compare differences between two groups, while one-way ANOVA was used for comparisons involving more than two groups. Spearman's correlation coefficients were utilized for correlation analyses. The Chi-square test
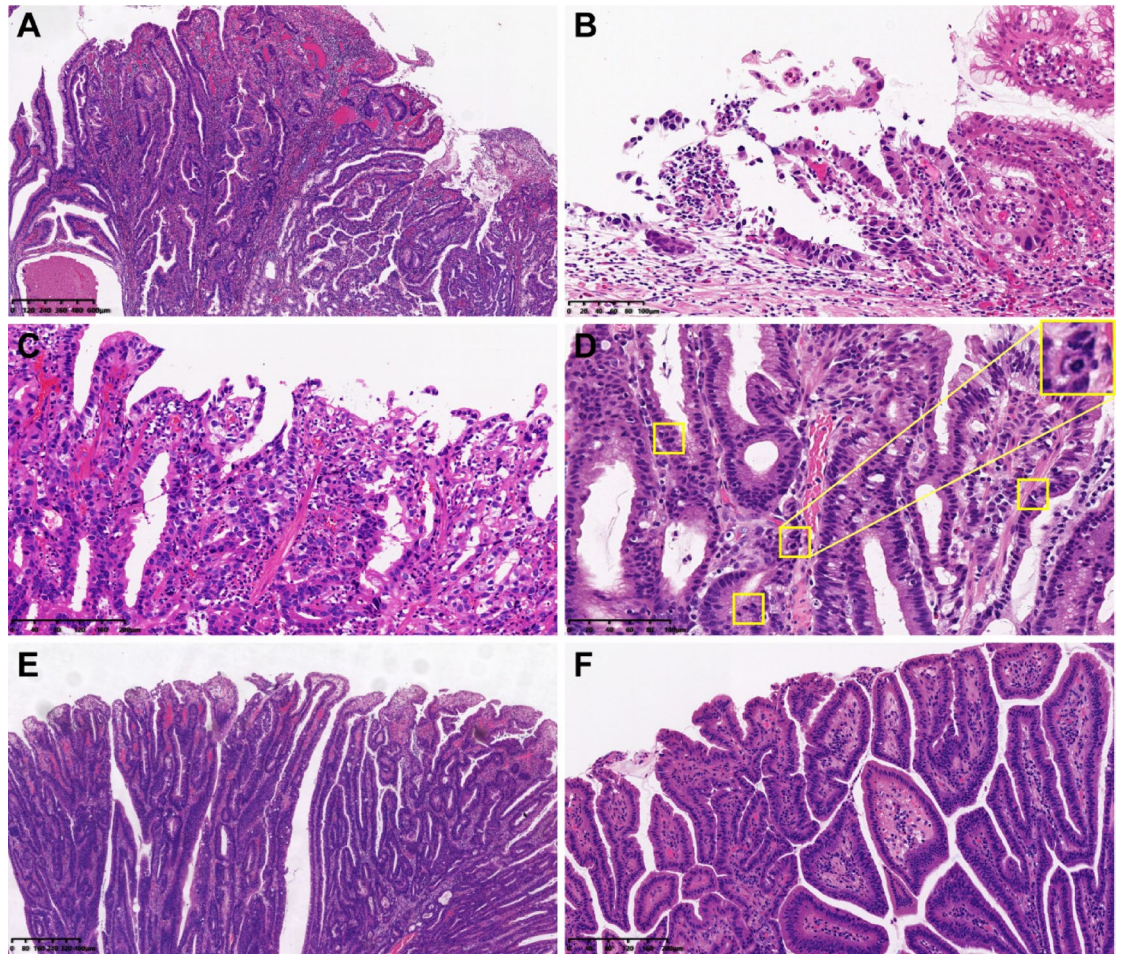
Fig. 2. Differences in histopathologic features between high-grade and low-grade EPGA. (**A**–**D**) Histopathological features of high-grade EPGA. (**A**) At low power field, high-grade EPGA displays complex villiform, papillary, serrated, and cleft-like structures with free-floating cell clusters on the surface and focal luminal necrosis. (**B**) At high power field, distinct single cells or small clusters of tumor cells are observed floating within glandular lumina or on the mucosal surface. (**C**) The nuclei are notably enlarged, hyperchromatic, and polymorphic, with prominent nucleoli; occasional tumor giant cells are also present. (**D**) Numerous mitotic figures are evident (yellow frames). (**E**, **F**) Histopathological features of low-grade EPGA. (**E**) At low power field, low-grade EPGA exhibits villiform papillary structures without complex serrated architecture or gland necrosis. (**F**) At high power field, there are no free-floating cell clusters on the surface. The tumor cells exhibit mild atypia, with slightly disordered polarity and infrequent mitotic figures.

and Fisher's exact test were applied to examine the association between clinicopathological characteristics and biomarker expression. Both univariate and multivariate logistic regression analyses were performed to identify independent risk factors for the development of EPGA and LVI, with odds ratios (OR) and 95% confidence intervals (95% CI) being estimated. The diagnostic efficacy of potential biomarkers was assessed through receiver operating characteristic (ROC) curve analysis. The area under the curve (AUC), along with 95% CI, was computed to evaluate predictive accuracy. Optimal cutoff values were identified using Youden's index (sensitivity + specificity − 1). Statistical significance was determined at a threshold of $P < 0.05$.

Results
Clinicopathological characteristics analysis
Table 1 presents the clinicopathological characteristics of EPGA and ETGA. Statistically significant differences were observed between the two groups in terms of tumor location ($P = 0.017$) and tumor differentiation ($P = 0.018$). Compared with ETGA, EPGA was more frequently located in the pylorus (58.6% vs. 44.8%, $P = 0.017$). At the same time, EPGA was significantly larger in size (median 2.15 cm, $P < 0.001$), exhibited a more elevated appearance (54.3% vs. 32.8%, $P = 0.001$), and demonstrated a higher incidence of ulcer formation (10.3% vs. 1.7%, $P = 0.010$). Furthermore, LVI was observed more frequently in EPGA than in ETGA (9.5% vs. 2.6%, $P = 0.050$). No significant differences were noted between the groups regarding age, sex, poorly differentiated carcinoma components, invasion depth, infiltration pattern, and LNM (all $P > 0.05$).

Characteristics	EPGA (n = 116)	ETGA (n = 116)	P-value
Age (years)	67 (59–71)	66 (59–71)	0.415
Sex			0.878
Male	89 (76.7%)	87 (75.0%)	
Female	27 (23.3%)	29 (25.0%)	
Location			0.017*
The cardia	20 (17.2%)	30 (25.9%)	
The fundus	4 (3.4%)	0 (0%)	
The corpus	24 (20.7%)	34 (29.3%)	
The pylorus	68 (58.6%)	52 (44.8%)	
Gross appearance			0.001*
Elevated	63 (54.3%)	38 (32.8%)	
Non-elevated	53 (45.7%)	78 (67.2%)	
Ulcer formation			0.010*
Present	12 (10.3%)	2 (1.7%)	
Absent	104 (89.7%)	114 (98.3%)	
Size (cm)	2.15 (1.60–3.18)	1.30 (0.90–2.10)	< 0.001*
Differentiation			0.018*
Moderately	66 (56.9%)	47 (40.5%)	
Well	50 (43.1%)	69 (59.5%)	
Poorly differentiated carcinoma components			0.247
Present	3 (2.6%)	0 (0%)	
Absent	113 (97.4%)	116 (100%)	
Invasion depth			0.141
Mucosa	94 (81.0%)	103 (88.8%)	
Submucosa	22 (19.0%)	13 (11.2%)	
Infiltrative pattern			0.124
INFa	96 (82.8%)	96 (82.8%)	
INFb	14 (12.1%)	19 (16.4%)	
INFc	6 (5.2%)	1 (0.9%)	
LVI			0.050*
Present	11 (9.5%)	3 (2.6%)	
Absent	105 (90.5%)	113 (97.4%)	
LNM			0.498
Present	2 (1.7%)	0 (0%)	
Absent	114 (98.3%)	116 (100%)	
MUC2			0.182
High expression	20 (17.2%)	12 (10.3%)	
Low expression	96 (82.8%)	104 (89.7%)	
MUC5AC			< 0.001*
High expression	80 (69.0%)	28 (24.1%)	
Low expression	36 (31.0%)	88 (75.9%)	
MUC6			0.110
High expression	55 (47.4%)	42 (36.2%)	
Low expression	61 (52.6%)	74 (63.8%)	
MSI status			0.005*
MSI-H	17 (14.7%)	4 (3.4%)	
MSI-L/MSS	99 (85.3%)	112 (96.6%)	
P53			0.147
Wild type	69 (59.5%)	57 (49.1%)	
Mutation type	47 (40.5%)	59 (50.9%)	
Ki-67	60% (50–70%)	60% (40–70%)	0.084

Table 1. Univariate analysis of the clinicopathological characteristics between EPGA and ETGA. *$p < 0.05$ with χ2 test or Fisher's exact test ($n < 5$). Lymphovascular invasion, LVI; Lymph node metastasis, LNM; Microsatellite instability, MSI; Microsatellite instability-high/low, MSI-H/MSI-L; Microsatellite stable, MSS.

Immunohistochemical analysis further revealed that the frequency of MSI-H was significantly greater in EPGA than in ETGA (14.7% vs. 3.4%, $P = 0.005$). Moreover, MUC5AC expression was significantly higher in EPGA compared to ETGA (69.0% vs. 24.1%, $P < 0.001$). However, no significant differences were observed in the expression of MUC2, MUC6, P53, and Ki-67 between the two groups (Fig. 3).

Independent distinguishing factors between EPGA and ETGA

In addition to the indicators identified as significant in the preceding univariate analysis, age and sex were incorporated into the multivariate logistic regression model to control for potential confounding bias. As detailed in Table 2, gross appearance (OR = 2.338, 95% CI = 1.157–4.724; $P = 0.018$), ulcer formation (OR = 7.645, 95% CI = 1.300–44.972; $P < 0.024$), tumor size (OR = 1.784, 95% CI = 1.355–2.350; $P < 0.001$), and MUC5AC expression (OR = 6.548, 95% CI = 3.329–12.881; $P < 0.001$) were identified as factors significantly associated with the histology of EPGA.

Subsequently, the diagnostic efficacy of these factors in distinguishing EPGA from ETGA cases was evaluated using receiver operating characteristic (ROC) curves, which yielded an area under the curve of 0.837 (95% CI
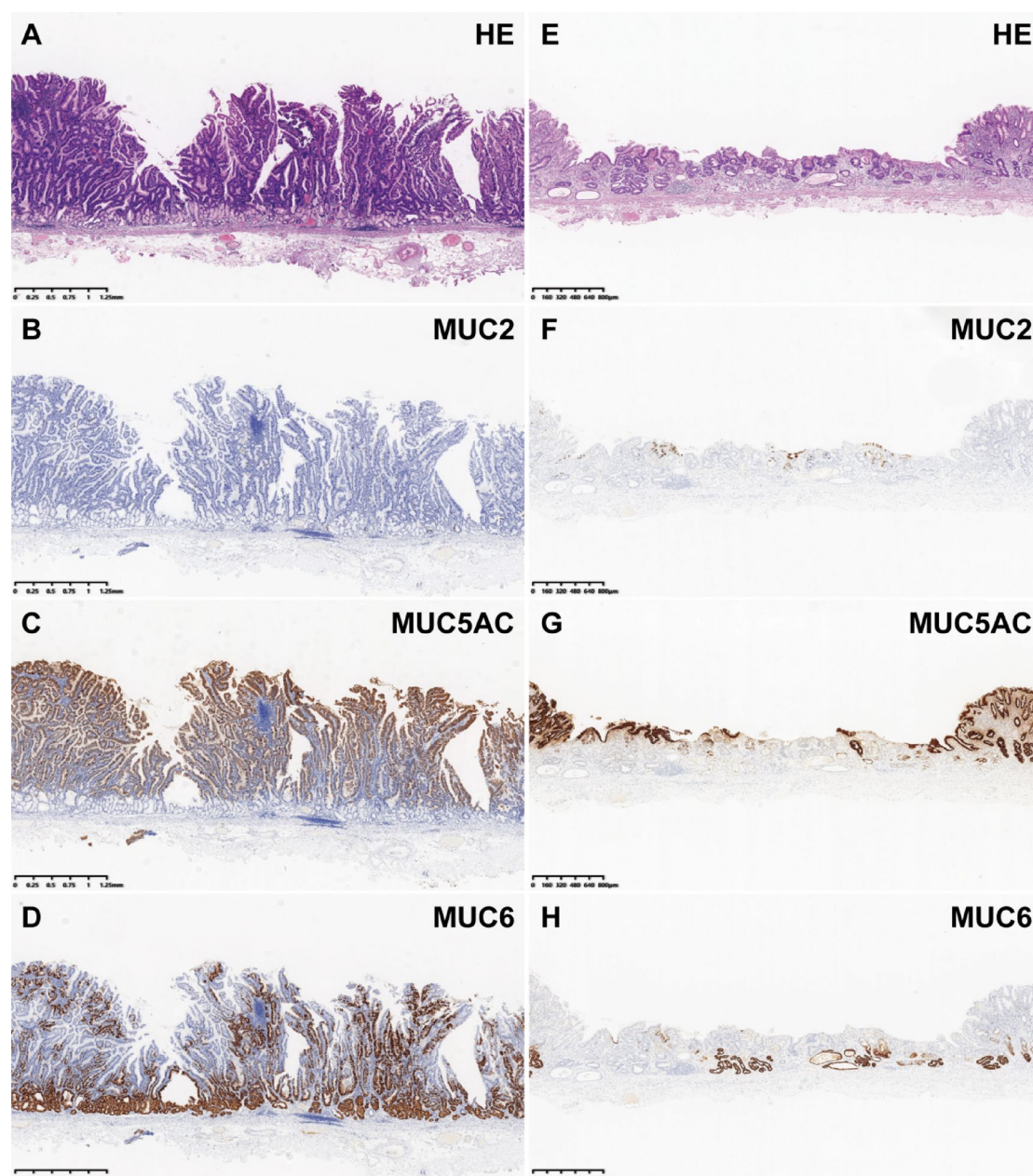

Fig. 3. Immunohistochemical staining of mucins in EPGA and ETGA. (**A–D**) The expression level of mucin in EGPA cases. (**E–H**) The expression level of mucin in ETGA cases. The expression of MUC5AC was significantly higher in EGPA than in ETGA, whereas the expression of MUC2 and MUC6 was similar between the two groups.

Variables	EPGA ($n = 116$)	ETGA ($n = 116$)	Odd ratio (95%CI)	P-value
Age (years)	67 (59–71)	66 (59–71)	1.015 (0.976–1.056)	0.454
Sex (Female)	27 (23.3%)	29 (25.0%)	0.657 (0.293–1.472)	0.307
Location				
The cardia	20 (17.2%)	30 (25.9%)	1 (reference)	0.101
The fundus	4 (3.4%)	0 (0%)	–	0.999
The corpus	24 (20.7%)	34 (29.3%)	0.935 (0.356–2.457)	0.891
The pylorus	68 (58.6%)	52 (44.8%)	2.361 (0.986–5.650)	0.054
Gross appearance (elevated)	63 (54.3%)	38 (32.8%)	2.338 (1.157–4.724)	0.018
Ulcer formation	12 (10.3%)	2 (1.7%)	7.645 (1.300–44.972)	0.024
Size (cm)	2.15 (1.60–3.18)	1.30 (0.90–2.10)	1.784 (1.355–2.350)	< 0.001
Differentiation (well)	50 (43.1%)	69 (59.5%)	0.751 (0.375–1.505)	0.419
MUC5AC (high)	80 (69.0%)	28 (24.1%)	6.548 (3.329–12.881)	< 0.001
MSI status (MSI-H)	17 (14.7%)	4 (3.4%)	2.691 (0.693–10.444)	0.152

Table 2. Multivariate logistic regression analysis of the clinicopathological characteristics between EPGA and ETGA.
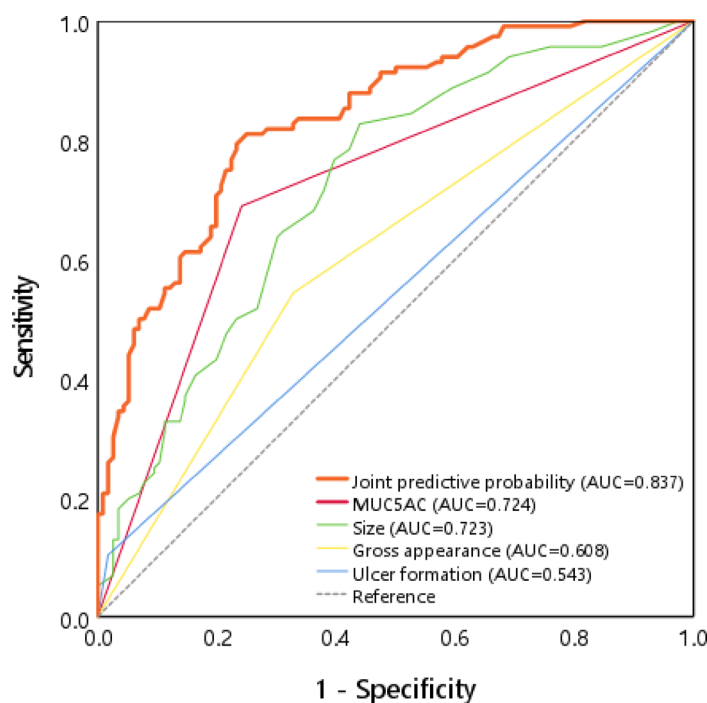

Fig. 4. ROC curves for the diagnostic performance of the joint predictive probability of MUC5AC expression, size, gross appearance and ulcer formation in EPGA.

= 0.787–0.887, $P < 0.001$), with a sensitivity of 80.2% and a specificity of 75.9% (Fig. 4). The optimal cutoff value for tumor size was determined to be 1.35 cm.

Comparison of clinicopathological characteristics among high-grade EPGA, low-grade EPGA, and ETGA

To enhance the understanding of the clinicopathological characteristics of EPGA, we stratified this tumor into high-grade and low-grade categories and conducted a comparative analysis with ETGA across three groups.

As illustrated in Table 3, the incidences of ulcer formation (16.1% vs. 1.7%, $P < 0.001$), submucosal invasion (27.4% vs. 11.2%, $P = 0.007$), moderately differentiated (67.7% vs. 40.5%, $P < 0.001$), high expression of MUC5AC (61.3% vs. 24.1%, $P < 0.001$), MSI-H (19.4% vs. 3.4%, $P < 0.001$), and the proportion of Ki-67 positivity (70% vs. 60%, $P = 0.001$) were all significantly elevated in high-grade EPGA compared to ETGA. Furthermore, high-grade EPGA exhibited a significantly larger tumor size than ETGA (median 2.25 cm vs. 1.30 cm, $P < 0.001$). The propensity for LVI was markedly more prevalent in high-grade EPGA than in ETGA (12.9% vs. 2.6%, $P = 0.010$), whereas no significant difference was observed when comparing low-grade EPGA to ETGA (5.6% vs. 2.6%,

Characteristics	High-grade EPGA ($n = 62$)	Low-grade EPGA ($n = 54$)	ETGA ($n = 116$)
Age (years)	67.5 (61.0–71.0)	66.5 (59.0–71.0)	66.0 (59.0–71.0)
Sex			
Male	50 (80.6%)	39 (72.2%)	87 (75.0%)
Female	12 (19.4%)	15 (27.8%)	29 (25.0%)
Location			
The cardia	11 (17.7%)	9 (16.7%)	30 (25.9%)
The fundus	2 (3.2%)	2 (3.7%)	0 (0%)
The corpus	14 (22.6%)	10 (18.5%)	34 (29.3%)
The pylorus	35 (56.5%)	33 (61.1%)	52 (44.8%)
Gross appearance			
Elevated	30 (48.4%)	33 (61.1%)#	38 (32.8%)
Non-elevated	32 (51.6%)	21 (38.9%)	78 (67.2%)
Ulcer formation			
Present	10 (16.1%)###	2 (3.7%)	2 (1.7%)
Absent	52 (83.9%)	52 (96.3%)	114 (98.3%)
Size (cm)	2.25 (1.60–3.50)#	2.05 (1.60–2.90)#	1.30 (0.90–2.10)
Differentiation			
Moderately	42 (67.7%)###	24 (44.4%)	47 (40.5%)
Well	20 (32.3%)	30 (55.6%)	69 (59.5%)
Invasion depth			
Mucosa	45 (72.6%)	49 (90.7%)	103 (88.8%)
Submucosa	17 (27.4%)###	5 (9.3%)	13 (11.2%)
Infiltrative pattern			
INFa	45 (72.6%)	51 (94.4%)	96 (82.8%)
INFb	11 (17.7%)	3 (5.6%)	19 (16.4%)
INFc	6 (9.7%)	0 (0%)	1 (0.9%)
LVI			
Present	8 (12.9%)#	3 (5.6%)	3 (2.6%)
Absent	54 (87.1%)	51 (94.4%)	113 (97.4%)
LNM			
Present	2 (3.2%)	0 (0%)	0 (0%)
Absent	60 (96.8%)	54 (100%)	116 (100%)
MUC2			
High expression	9 (14.5%)	11 (20.4%)	12 (10.3%)
Low expression	53 (85.5%)	43 (79.6%)	104 (89.7%)
MUC5AC			
High expression	38 (61.3%)#	42 (77.8%)#	28 (24.1%)
Low expression	24 (38.7%)	12 (22.2%)	88 (75.9%)
MUC6			
High expression	25 (40.3%)	30 (55.6%)#	42 (36.2%)
Low expression	37 (59.7%)	24 (44.4%)	74 (63.8%)
MSI status			
MSI-H	12 (19.4%)#	5 (9.3%)	4 (3.4%)
MSI-L/MSS	50 (80.6%)	49 (90.7%)	112 (96.6%)
P53			
Wild type	28 (45.2%)	41 (75.9%)#	57 (49.1%)
Mutation type	34 (54.8%)##	13 (24.1%)	59 (50.9%)
Ki-67	70% (60–70%)###	60% (40–70%)	60% (40–70%)

Table 3. Comparison of clinicopathological characteristics among high-grade EPGA, low-grade EPGA, and ETGA. #$p < 0.05$ compared with the ETGA group. ##$p < 0.05$ compared with the low-grade EPGA group. Lymphovascular invasion, LVI; Lymph node metastasis, LNM; Microsatellite instability, MSI; Microsatellite instability-high/low, MSI-H/MSI-L; Microsatellite stable, MSS.

$P = 0.383$). Additionally, a notable disparity was observed in the frequency of aberrant P53 expression between high-grade and low-grade EPGA (54.8% vs. 24.1%, $P = 0.001$). These results suggest that high-grade EPGA is characterized by aggressive tumor behavior and distinct molecular features, whereas low-grade EPGA shares clinicopathological characteristics with ETGA.

Comparison of clinicopathological characteristics between MUC5AC high-expression EPGA and MUC5AC low-expression EPGA

EPGA was further divided into groups based on MUC5AC expression levels. As shown in Table 4, elevated appearance was more frequent in MUC5AC high-expression EPGA compared to low-expression EPGA (61.3% vs. 38.9%, $P = 0.029$), while LVI was more prevalent in MUC5AC low-expression EPGA (19.4% vs. 5.0%, $P = 0.034$). Additionally, MUC5AC expression demonstrated a positive correlation with MUC6 expression ($P = 0.017$). No significant differences were observed between the groups regarding age, sex, tumor location, tumor size, tumor differentiation, ulcer formation, invasion depth, infiltration pattern, LNM, MUC2 expression, P53 expression, Ki-67 expression, and MSI status (all $P > 0.05$).

Risk factors for LVI in EGC

In the univariate logistic regression analysis presented in Table 5, several significant risk factors for LVI in 232 cases of EGC were identified. These factors included ulcer formation, tumor size, high-grade papillary histology, well-differentiated tumors, submucosal invasion, an infiltrative pattern (INFa/INFb), MSI-H phenotype, and Ki-67 expression (all $P < 0.05$). Further analysis using multivariate logistic regression revealed that submucosal invasion (OR = 26.132, 95% CI = 4.193–162.854; $P < 0.001$) and the MSI-H phenotype (OR = 10.179, 95% CI = 1.419–72.988; $P = 0.021$) were independent risk factors for LVI in EGC.

Discussion

In this study, we conducted a comprehensive analysis of the clinicopathological characteristics and mucin expression profiles of EPGA. Our findings identified four factors that differentiate EPGA from ETGA: tumor size, ulcer formation, gross appearance, and MUC5AC expression. ROC curve analysis demonstrated that the joint predictive power of these factors effectively discriminated between EPGA and ETGA. Furthermore, subgroup analyses of EPGA revealed the following insights: (1) high-grade EPGA exhibited highly aggressive tumor behavior and distinct molecular features, whereas low-grade EPGA shared clinicopathological attributes with ETGA; (2) there is a positive correlation between MUC5AC and MUC6 expression. Additionally, we found that LVI was closely associated with MSI status and invasion depth in EGC.

MUC5AC, recognized as a critical molecular marker for GC, has been extensively investigated. Numerous studies have reported that MUC5AC expression is either absent or reduced in certain advanced GC cases[41–43]. However, the expression level of MUC5AC in EGC, particularly in EPGA, remains insufficiently characterized. In this study, we demonstrated that the expression of MUC5AC in EPGA was significantly higher than in ETGA ($P < 0.001$). Moreover, ROC curve analysis indicated that MUC5AC expression effectively distinguished between EPGA and ETGA (AUC = 0.724, sensitivity = 69.0%, specificity = 75.9%), suggesting the potential of MUC5AC expression as an effective diagnostic marker for differentiating EPGA from ETGA. Alterations in mucin expression are recognized as molecular markers indicative of malignant transformation in the gastric mucosa[24]. Numerous studies have reported the expression of MUC5AC is characteristically decreased during gastric carcinogenesis[44–46]. Consistent with these findings, our subgroup analysis found that LVI was significantly more prevalent in EPGA with low MUC5AC expression ($P = 0.034$), suggesting a potential tumor suppressor role for MUC5AC. Additionally, we revealed a positive correlation between the expression of MUC5AC and MUC6 in EPGA ($P = 0.017$). Both MUC5AC and MUC6 are recognized as markers for gastric phenotype GC[24]. The expression of phenotypic markers in GC is associated with clinicopathological variables, such as cancer survival[47–49]. Several studies have reported that the downregulation of MUC6 facilitates the progression of GC at the molecular level[49–52]. In contrast, other researches suggest that MUC5AC may serve as a clinically valuable marker for predicting malignancy outcomes in GC[47,48]. However, the precise mechanisms by which MUC5AC operates in GC remain to be elucidated.

According to the treatment guidelines issued by the Japanese Gastric Cancer Association, EPGA is more frequently observed as the 0-IIa type, characterized by a superficially elevated appearance[53]. Consistent with these guidelines, our research demonstrated that EPGA was associated with a larger median size (2.15 cm) and a more pronounced elevated appearance (54.3% vs. 32.8%, $P = 0.001$) compared to ETGA. However, the diagnostic efficacy of these two factors in distinguishing between EPGA and ETGA is limited, with the AUC values of 0.723 (sensitivity = 82.8%, specificity = 56.0%) and 0.608 (sensitivity = 55.1%, specificity = 67.2%), respectively. We propose that the discrepancy in tumor size and gross appearance between EPGA and ETGA may be attributed to their distinct growth patterns. EPGA is characterized by exophytic papillary structures that facilitate vertical expansion within the mucosal layer, resulting in larger elevated lesions. In contrast, ETGA primarily exhibits horizontal infiltrative growth with limited volumetric expansion.

High-grade EPGA displayed markedly aggressive tumor behavior and distinct molecular characteristics, unlike low-grade EPGA, which shared clinicopathological features with ETGA, as evidenced by both current and previous studies[12]. Our comparative analysis among the three groups revealed that high-grade EPGA had significantly higher rates of submucosal invasion (27.4%), ulcer formation (16.1%), and a diffuse infiltrative pattern (9.7%) compared to both low-grade EPGA and ETGA. The higher incidence of submucosal invasion in high-grade EPGA indicates aggressive biological behavior, a finding supported by multivariate logistic regression analysis (OR = 25.227, 95% CI = 4.017–158.432; $P < 0.001$). Importantly, our research also identified that high-grade papillary architecture was significantly associated with LVI, underscoring the importance of architectural complexity in distinguishing high-grade from low-grade EPGA in prognostic assessments. Contrary to previous

Characteristics	All ($n = 116$)	MUC5AC		P-value
		High expression ($n = 80$)	Low expression ($n = 36$)	
Age (years)	67 (59–71)	66.0 (58.3–71.0)	67.5 (61.5–72.0)	0.527
Sex				0.637
Male	89	60 (75.0%)	29 (80.6%)	
Female	27	20 (25.0%)	7 (19.4%)	
Location				0.167
The cardia	20	13 (16.3%)	7 (19.4%)	
The fundus	4	4 (5.0%)	0 (0%)	
The corpus	24	20 (25.0%)	4 (11.1%)	
The pylorus	68	43 (53.8%)	25 (69.4%)	
Gross appearance				0.029*
Elevated	63	49 (61.3%)	14 (38.9%)	
Non-elevated	53	31 (38.8%)	22 (61.1%)	
Ulcer formation				0.186
Present	12	6 (7.5%)	6 (16.7%)	
Absent	104	74 (92.5%)	30 (83.3%)	
Invasion depth				1.000
Mucosa	94	65 (81.3%)	29 (80.6%)	
Submucosa	22	15 (18.8%)	7 (19.4%)	
Size (cm)	2.15 (1.60–3.18)	2.00 (1.53–3.08)	2.40 (1.63–3.45)	0.219
Differentiation				0.686
Moderately	66	47 (59.7%)	19 (52.8%)	
Well	50	33 (41.3%)	17 (47.2%)	
Infiltrative pattern				0.461
INFa	96	68 (85.0%)	28 (77.8%)	
INFb	14	9 (11.3%)	5 (13.9%)	
INFc	6	3 (3.8%)	3 (8.3%)	
LVI				0.034*
Present	11	4 (5.0%)	7 (19.4%)	
Absent	105	76 (95.0%)	29 (80.6%)	
LNM				0.094
Present	2	0 (0%)	2 (5.6%)	
Absent	114	80 (100%)	34 (94.4%)	
Histology				0.071
High-grade	62	38 (47.5%)	24 (66.7%)	
Low-grade	54	42 (52.5%)	12 (33.3%)	
MUC2				0.184
High expression	20	11 (13.8%)	9 (25.0%)	
Low expression	96	69 (86.3%)	27 (75.0%)	
MUC6				0.017*
High expression	55	44 (55.0%)	11 (30.6%)	
Low expression	61	36 (45.0%)	25 (69.4%)	
MSI status				0.088
MSI-H	17	15 (18.8%)	2 (5.6%)	
MSI-L/MSS	99	65 (81.3%)	34 (94.4%)	
Ki-67 (positive index)	60% (50%~70%)	60% (50%~70%)	65% (50%~70%)	0.552
P53				0.414
Wild type	69	50 (62.5%)	19 (52.8%)	
Mutation type	47	30 (37.5%)	17 (47.2%)	

Table 4. Comparison of clinicopathological characteristics between MUC5AC high-expression EPGA and MUC5AC low-expression EPGA. *$p < 0.05$ with χ2 test or Fisher's exact test ($n < 5$). Lymphovascular invasion, LVI; Lymph node metastasis, LNM; Microsatellite instability, MSI; Microsatellite instability-high/low, MSI-H/ MSI-L; Microsatellite stable, MSS.

Characteristics	Univariate Analysis		Multivariate Analysis	
	OR (95% CI)	*P*-value	OR (95% CI)	*P*-value
Age (years)	1.004 (0.943–1.069)	0.898		
Sex (Female)	0.849 (0.228–3.158)	0.807		
Location				
The cardia	1 (reference)	0.642		
The fundus	0.000 (0.000~)	0.999		
The corpus	3.630 (0.392–33.592)	0.256		
The pylorus	3.973 (0.490–32.223)	0.196		
Gross appearance (elevated)	1.792 (0.601–5.341)	0.295		
Ulcer formation	5.132 (1.249–21.091)	0.023*	0.663 (0.083–5.279)	0.697
Size (cm)	1.320 (1.033–1.687)	0.026*	0.965 (0.634–1.469)	0.869
Histology			1 (reference)	
ETGA	1 (reference)	0.039		0.211
Low-grade EPGA	2.216 (0.432–11.355)	0.340	6.940 (0.741–65.001)	0.090
High-grade EPGA	5.580 (1.424–21.871)	0.014*	3.779 (0.576–24.794)	0.166
Differentiation (Well)	0.065 (0.008–0.507)	0.009*	0.116 (0.012–1.093)	0.060
Poorly differentiated carcinoma component	8.308 (0.706–97.712)	0.092		
Submucosal invasion	19.300 (5.629–66.169)	< 0.001*	26.132 (4.193–162.854)	< 0.001*
Infiltrative pattern				
INFa	1 (reference)	0.009	1 (reference)	0.361
INFb	5.873 (1.836–18.787)	0.003*	2.607 (0.449–15.135)	0.286
INFc	4.405 (0.465–41.687)	0.196	0.464 (0.029–7.403)	0.587
LNM	16.692 (0.987–282.220)	0.051		
MUC2 (high)	1.044 (0.223–4.900)	0.956		
MUC5AC (high)	1.158 (0.393–3.414)	0.790		
MUC6 (high)	1.422 (0.482–4.195)	0.523		
MSI status (MSI-H)	4.729 (1.340–16.686)	0.016*	10.179 (1.419–72.988)	0.021*
P53 (mutation type)	1.202 (0.408–3.543)	0.739		
Ki-67	74.463 (1.234–4492.564)	0.039*	11.235 (0.048–2619.731)	0.384

Table 5. Risk factors of LVI in EGC. *$p < 0.05$ with $\chi2$ test or Fisher's exact test ($n < 5$). Lymph node metastasis, LNM; Microsatellite instability-high, MSI-H.

reports[12], our cohorts did not exhibit statistically significant differences in tumor size, LVI, and LNM between low-grade and high-grade EPGA. This discrepancy may be due to the limited sample size and potential selection bias. Additionally, the mutant P53 protein is markedly expressed in early differentiated gastric adenocarcinoma, serving as an auxiliary marker for the diagnosis of EGC[54]. In low-grade adenocarcinoma, the protein exhibits weak positivity (wild type), whereas in high-grade adenocarcinoma, it is either strongly positive or negative (mutation type)[55], consistent with our findings. The distinct expression patterns of the mutant P53 protein in high-grade and low-grade EPGA indicate different genetic alterations[55]. Therefore, our findings support the notion that EPGA is heterogeneous, and high-grade EPGA should be considered a specific variant warranting increased attention.

The assessment of microsatellite instability (MSI) in our study found that EPGA exhibited a significantly higher prevalence of the microsatellite instability-high (MSI-H) phenotype compared to ETGA ($P = 0.005$). The MSI phenotype is a molecular subtype that is recognized in GC[56,57], and the proportion of MSI-H GCs has been related to earlier tumor stages[58–62]. Additionally, researches reported that MSI was more frequently observed in PGA and solid poorly differentiated adenocarcinoma[57,63,64]. A high level of MSI correlates with an increased mutation rate[65]. MSI-H GC is predominantly attributed to the silencing of the mutL homolog 1 (MLH1) gene, resulting from CpG island hypermethylation[66]. Guo et al. have demonstrated that the methylation-induced silencing of the hMLH1 gene is an early event that precedes the manifestation of MSI in the carcinogenesis of PGA[67]. Therefore, EPGA should be regarded as a type of MSI-H GC. Moreover, certain studies have indicated that MSI-H tumors are associated with a favorable prognosis, and MSI status may serve as a predictive marker for chemotherapy responsiveness in stage II/III GC[68,69]. However, MSI does not appear to have a prognostic role in EGC[70,71]. In our study, we identified MSI as a significant risk factor for the occurrence of LVI in EGC ($P = 0.019$).

Several limitations of our study merit careful consideration. Firstly, the retrospective design may introduce sample selection bias, underscoring the necessity for further validation of our findings through the collection

of additional cases. Secondly, due to the low incidence of EPGA, the control group in our study was relatively small and maintained a 1:1 ratio, with limited tumor types represented. This limitation highlights the need for future large-scale, multicenter studies to substantiate our current results. Thirdly, although the expression levels of MUC5AC and MMR proteins were significantly higher in EPGA compared to ETGA, further validation of the immunohistochemical markers for MUC5AC, MMR, and other related genes is required through additional molecular investigations.

Conclusion

This study demonstrated that early gastric papillary adenocarcinoma, particularly high-grade EPGA, exhibits a higher degree of malignancy compared to other types of gastric differentiated adenocarcinoma. The high expression of MUC5AC is highly indicative of EPGA, offering valuable insights for its diagnosis. Furthermore, MSI was identified as being associated with the presence of LVI in EGC.

Data availability

The data were obtained in Department of pathology, the Second Hospital of Shandong University. The datasets used and during the current study are available from the corresponding authors on reasonable request.

References

1. Sung, H. et al. Global cancer statistics 2020: GLOBOCAN estimates of incidence and mortality worldwide for 36 cancers in 185 countries. *Cancer J. Clin.* **71**(3), 209–249. https://doi.org/10.3322/caac.21660 (2021).
2. Conti, C. B. et al. Early gastric cancer: Update on prevention, diagnosis and treatment. *Int. J. Environ. Res. Public. Health* **20**(3), 2149. https://doi.org/10.3390/ijerph20032149 (2023).
3. Nagtegaal, I. D. et al. The 2019 WHO classification of tumours of the digestive system. *Histopathology* **76**(2), 182–188. https://doi.org/10.1111/his.13975 (2020).
4. Japanese Gastric Cancer Association. Japanese classification of gastric carcinoma: 3rd english edition. *Gastric Cancer* **14**(2), 101–112. https://doi.org/10.1007/s10120-011-0041-5 (2011).
5. Quach, D. T., Hiyama, T. & Gotoda, T. Identifying high-risk individuals for gastric cancer surveillance from Western and Eastern perspectives: Lessons to learn and possibility to develop an integrated approach for daily practice. *World J. Gastroenterol.* **25**(27), 3546–3562. https://doi.org/10.3748/wjg.v25.i27.3546 (2019).
6. Xuan, Z. X., Ueyama, T., Yao, T. & Tsuneyoshi, M. Time trends of early gastric carcinoma. A clinicopathological analysis of 2846 cases. *Cancer* **72**(10), 2889–2894. https://doi.org/10.1002/1097-0142(19931115)72:10%3C2889::aid-cncr2820721006%3E3.0.co;2-j (1993).
7. Lee, H. H., Song, K. Y., Park, C. H. & Jeon, H. M. Undifferentiated-type gastric adenocarcinoma: Prognostic impact of three histological types. *World J. Surg. Oncol.* **10**, 254. https://doi.org/10.1186/1477-7819-10-254 (2012).
8. Koseki, K. et al. Distinction of differentiated type early gastric carcinoma with gastric type mucin expression. *Cancer* **89**(4), 724–732 (2000).
9. Yasuda, K., Adachi, Y., Shiraishi, N., Maeo, S. & Kitano, S. Papillary adenocarcinoma of the stomach. *Gastric Cancer* **3**(1), 33–38. https://doi.org/10.1007/pl00011687 (2000).
10. Chen, J., Cui, X., Wu, H. & Zhou, C. Case report: A rare case of very well-differentiated gastric adenocarcinoma of gastric type with a lymphovascular invasion. *Front. Oncol.* **14**, 1396281. https://doi.org/10.3389/fonc.2024.1396281 (2024).
11. Zuo, Z. et al. Endoscopic and clinicopathological features of early gastric papillary adenocarcinoma. *Front. Oncol.* **14**, 1456520. https://doi.org/10.3389/fonc.2024.1456520 (2024).
12. Cheng, Y. et al. High-grade papillary early gastric carcinoma with high risk for lymph node metastasis and poor prognosis: A clinicopathological study of 96 cases among 1136 consecutive radical gastrectomies. *Am. J. Surg. Pathol.* **45**(12), 1661–1668. https://doi.org/10.1097/PAS.0000000000001759 (2021).
13. Kim, T. S. et al. Endoscopic submucosal dissection for papillary adenocarcinoma of the stomach: Low curative resection rate but favorable long-term outcomes after curative resection. *Gastric Cancer* **22**(2), 363–368. https://doi.org/10.1007/s10120-018-0857-3 (2019).
14. Sekiguchi, M. et al. Clinical significance of a papillary adenocarcinoma component in early gastric cancer: A single-center retrospective analysis of 628 surgically resected early gastric cancers. *J. Gastroenterol.* **50**(4), 424–434. https://doi.org/10.1007/s00535-014-0991-6 (2015).
15. Yu, H. et al. Worse prognosis in papillary, compared to tubular, early gastric carcinoma. *J. Cancer* **8**(1), 117–123. https://doi.org/10.7150/jca.17326 (2017).
16. Min, B. H. et al. Lymphovascular invasion and lymph node metastasis rates in papillary adenocarcinoma of the stomach: Implications for endoscopic resection. *Gastric cancer*. **21**(4), 680–688. https://doi.org/10.1007/s10120-017-0785-7 (2018).
17. Lee, H. J. et al. Endoscopic submucosal dissection for papillary adenocarcinoma of the stomach: Is it really safe? *Gastric Cancer* **20**(6), 978–986. https://doi.org/10.1007/s10120-017-0709-6 (2017).
18. Devine, P. L. & McKenzie, I. F. Mucins: Structure, function, and associations with malignancy. *BioEssays* **14**(9), 619–625. https://doi.org/10.1002/bies.950140909 (1992).
19. Andrianifahanana, M., Moniaux, N. & Batra, S. K. Regulation of mucin expression: Mechanistic aspects and implications for cancer and inflammatory diseases. *Biochim. Biophys. Acta* **1765**(2), 189–222. https://doi.org/10.1016/j.bbcan.2006.01.002 (2006).
20. Silva, E. et al. Mucins as key molecules for the classification of intestinal metaplasia of the stomach. *Virchows Arch.* **440**(3), 311–317. https://doi.org/10.1007/s004280100531 (2002).
21. Reis, C. A., David, L., Seixas, M., Burchell, J. & Sobrinho-Simões, M. Expression of fully and under-glycosylated forms of MUC1 mucin in gastric carcinoma. *Int. J. Cancer* **79**(4), 402–410. https://doi.org/10.1002/(sici)1097-0215(19980821)79:4%3C402::aid-ijc16%3E3.0.co;2-6 (1998).
22. Corfield, A. P. et al. Mucins and mucosal protection in the Gastrointestinal tract: New prospects for mucins in the pathology of Gastrointestinal disease. *Gut* **47**(4), 589–594. https://doi.org/10.1136/gut.47.4.589 (2000).
23. Lupan, I., Bintintan, V., Deleanu, D. & Samasca, G. Epigenetic regulation of DNA methylation and RNA interference in gastric cancer: A 2024 update. *Biomedicines* **12**(9), 2001. https://doi.org/10.3390/biomedicines12092001 (2024).
24. Battista, S., Ambrosio, M. R., Limarzi, F., Gallo, G. & Saragoni, L. Molecular alterations in gastric preneoplastic lesions and early gastric cancer. *Int. J. Mol. Sci.* **22**(13), 6652. https://doi.org/10.3390/ijms22136652 (2021).
25. Wakatsuki, K. et al. Clinicopathological and prognostic significance of mucin phenotype in gastric cancer. *J. Surg. Oncol.* **98**(2), 124–129. https://doi.org/10.1002/jso.21093 (2008).

26. Roh, J. H. et al. Micropapillary carcinoma of stomach: A clinicopathologic and immunohistochemical study of 11 cases. *Am. J. Surg. Pathol.* **34**(8), 1139–1146. https://doi.org/10.1097/PAS.0b013e3181e7043b (2010).

27. Uesugi, N. et al. Clinicopathological and molecular stability and methylation analyses of gastric papillary adenocarcinoma. *Pathology* **49**(6), 596–603. https://doi.org/10.1016/j.pathol.2017.07.004 (2017).

28. Huang, Q. et al. Differences in clinicopathology of early gastric carcinoma between proximal and distal location in 438 Chinese patients. *Sci. Rep.* **5**, 13439. https://doi.org/10.1038/srep13439 (2015).

29. The Paris endoscopic classification of superficial neoplastic lesions: Esophagus, stomach, and colon: November 30 to December 1. *Gastrointestinal endoscopy*, 58(6 Suppl), S3–S43 (2002). https://doi.org/10.1016/s0016-5107(03)02159-x (2003).

30. Li, N. et al. Prognostic evaluation of Nanog, Oct4, Sox2, PCNA, Ki67 and E-cadherin expression in gastric cancer. *Med. Oncol. (Northwood Lond. Engl.)* **32**(1), 433. https://doi.org/10.1007/s12032-014-0433-6 (2015).

31. Marano, L. et al. Surgical management of advanced gastric cancer: An evolving issue. *Eur. J. Surg. Oncol.* **42**(1), 18–27. https://doi.org/10.1016/j.ejso.2015.10.016 (2016).

32. Kim, H. et al. Growth patterns of signet ring cell carcinoma of the stomach for endoscopic resection. *Gut Liver* **9**(6), 720–726. https://doi.org/10.5009/gnl14203 (2015).

33. Shin, S. Y. et al. Clinicopathologic features of submucosal papillary gastric cancer differ from those of other differentiated-type histologies. *Gut Liver* **15**(1), 44–52. https://doi.org/10.5009/gnl19328 (2021).

34. Kushima, R. The updated WHO classification of digestive system tumours-gastric adenocarcinoma and dysplasia. Die Aktuelle WHO-Klassifikation der tumoren des Verdauungstrakts—Dysplasie und adenokarzinom des Magens. *Der Pathologe.* **43**(1), 8–15. https://doi.org/10.1007/s00292-021-01023-7 (2022).

35. Nakashima, Y. et al. Nuclear atypia grading score is a useful prognostic factor in papillary gastric adenocarcinoma. *Histopathology* **59**(5), 841–849. https://doi.org/10.1111/j.1365-2559.2011.04035.x (2011).

36. Fukai, S. et al. Down-regulation of stimulator of interferon genes (STING) expression and CD8 + T-cell infiltration depending on HER2 heterogeneity in HER2-positive gastric cancer. *Gastric Cancer* **26**(6), 878–890. https://doi.org/10.1007/s10120-023-01417-x (2023).

37. Shin, J. S., Tut, T. G., Yang, T. & Lee, C. S. Radiotherapy response in microsatellite instability related rectal cancer. *Korean J. Pathol.* **47**(1), 1–8. https://doi.org/10.4132/KoreanJPathol.2013.47.1.1 (2013).

38. Arai, T., Komatsu, A., Kanazawa, N., Nonaka, K. & Ishiwata, T. Clinicopathological and molecular characteristics of gastric papillary adenocarcinoma. *Pathol. Int.* **73**(8), 358–366. https://doi.org/10.1111/pin.13345 (2023).

39. Boland, C. R. et al. A National cancer Institute workshop on microsatellite instability for cancer detection and Familial predisposition: Development of international criteria for the determination of microsatellite instability in colorectal cancer. *Cancer Res.* **58**(22), 5248–5257 (1998).

40. Shields, P. G. et al. Smoking cessation, version 3.2022, NCCN clinical practice guidelines in oncology. *J. Natl. Compr. Canc. Netw.* **21**(3), 297–322. https://doi.org/10.6004/jnccn.2023.0013 (2023).

41. Reis, C. A. et al. Immunohistochemical study of MUC5AC expression in human gastric carcinomas using a novel monoclonal antibody. *Int. J. Cancer* **74**(1), 112–121. https://doi.org/10.1002/(sici)1097-0215(19970220)74:1%3C112::aid-ijc19%3E3.0.co;2-h (1997).

42. Carrato, C. et al. Differential apomucin expression in normal and neoplastic human gastrointestinal tissues. *Gastroenterology* **107**(1), 160–172. https://doi.org/10.1016/0016-5085(94)90073-6 (1994).

43. Ho, S. B. et al. Mucin gene expression in normal, preneoplastic, and neoplastic human gastric epithelium. *Cancer Res.* **55**(12), 2681–2690 (1995).

44. Kocer, B. et al. Prognostic significance of mucin expression in gastric carcinoma. *Dig. Dis. Sci.* **49**(6), 954–964. https://doi.org/10.1023/b:ddas.0000034554.96191.66 (2004).

45. Suh, Y. S. et al. The combined expression of metaplasia biomarkers predicts the prognosis of gastric cancer. *Ann. Surg. Oncol.* **19**(4), 1240–1249. https://doi.org/10.1245/s10434-011-2125-1 (2012).

46. Wang, J. Y. et al. Role of MUC1 and MUC5AC expressions as prognostic indicators in gastric carcinomas. *J. Surg. Oncol.* **83**(4), 253–260. https://doi.org/10.1002/jso.10222 (2003).

47. Mizoshita, T. et al. Expression of CDX2 and the phenotype of advanced gastric cancers: Relationship with prognosis. *J. Cancer Res. Clin. Oncol.* **129**(12), 727–734. https://doi.org/10.1007/s00432-003-0499-6 (2003).

48. Tajima, Y. et al. Gastric and intestinal phenotypic marker expression in gastric carcinomas and its prognostic significance: Immunohistochemical analysis of 136 lesions. *Oncology* **61**(3), 212–220. https://doi.org/10.1159/000055377 (2001).

49. Zheng, H. et al. MUC6 down-regulation correlates with gastric carcinoma progression and a poor prognosis: An immunohistochemical study with tissue microarrays. *J. Cancer Res. Clin. Oncol.* **132**(12), 817–823. https://doi.org/10.1007/s00432-006-0135-3 (2006).

50. Shiratsu, K., Higuchi, K. & Nakayama, J. Loss of gastric gland mucin-specific O-glycan is associated with progression of differentiated-type adenocarcinoma of the stomach. *Cancer Sci.* **105**(1), 126–133. https://doi.org/10.1111/cas.12305 (2014).

51. Molinari, C. et al. Early gastric cancer: Identification of molecular markers able to distinguish submucosa-penetrating lesions with different prognosis. *Gastric Cancer* **24**(2), 392–401. https://doi.org/10.1007/s10120-020-01135-8 (2021).

52. Shi, D. & Xi, X. X. Regulation of MUC6 methylation correlates with progression of gastric cancer. *Yonsei Med. J.* **62**(11), 1005–1015. https://doi.org/10.3349/ymj.2021.62.11.1005 (2021).

53. Japanese Gastric Cancer Association. Japanese gastric cancer treatment guidelines 2014 (ver. 4). *Gastric Cancer* **20**(1), 1–19. https://doi.org/10.1007/s10120-016-0622-4 (2017).

54. Prass, K. et al. Hypoxia-induced stroke tolerance in the mouse is mediated by erythropoietin. *Stroke* **34**(8), 1981–1986. https://doi.org/10.1161/01.STR.0000080381.76409.B2 (2003).

55. Tang, M., Liu, P. J., Yue, B., Yang, X. T. & Chen, G. Y. The correlation between mutant p53 protein expression and cell atypia in early differentiated gastric adenocarcinoma. *Cancer Manag. Res.* **13**, 4129–4134. https://doi.org/10.2147/CMAR.S305382 (2021).

56. Cancer genome atlas research network comprehensive molecular characterization of gastric adenocarcinoma. *Nature* **513**(7517), 202–209. https://doi.org/10.1038/nature13480 (2014).

57. Cristescu, R. et al. Molecular analysis of gastric cancer identifies subtypes associated with distinct clinical outcomes. *Nat. Med.* **21**(5), 449–456. https://doi.org/10.1038/nm.3850 (2015).

58. An, J. Y. et al. Microsatellite instability in sporadic gastric cancer: Its prognostic role and guidance for 5-FU based chemotherapy after R0 resection. *Int. J. Cancer* **131**(2), 505–511. https://doi.org/10.1002/ijc.26399 (2012).

59. Choi, Y. Y. et al. Is microsatellite instability a prognostic marker in gastric cancer? A systematic review with meta-analysis. *J. Surg. Oncol.* **110**(2), 129–135. https://doi.org/10.1002/jso.23618 (2014).

60. Kim, S. Y. et al. The benefit of microsatellite instability is attenuated by chemotherapy in stage II and stage III gastric cancer: Results from a large cohort with subgroup analyses. *Int. J. Cancer.* **137**(4), 819–825. https://doi.org/10.1002/ijc.29449 (2015).

61. Polom, K. et al. The pattern of lymph node metastases in microsatellite unstable gastric cancer. *Eur. J. Surg. Oncol.* **43**(12), 2341–2348. https://doi.org/10.1016/j.ejso.2017.09.007 (2017).

62. Polom, K. et al. Meta-analysis of microsatellite instability in relation to clinicopathological characteristics and overall survival in gastric cancer. *Br. J. Surg.* **105**(3), 159–167. https://doi.org/10.1002/bjs.10663 (2018).

63. Marrelli, D. et al. Strong prognostic value of microsatellite instability in intestinal type non-cardia gastric cancer. *Ann. Surg. Oncol.* **23**(3), 943–950. https://doi.org/10.1245/s10434-015-4931-3 (2016).

64. Arai, T. et al. Frequent microsatellite instability in papillary and solid-type, poorly differentiated adenocarcinomas of the stomach. *Gastric Cancer* **16**(4), 505–512. https://doi.org/10.1007/s10120-012-0226-6 (2013).
65. Li, Z., Pearlman, A. & Hsieh, H. DNA mismatch repair and the DNA damage response. *DNA Repair.* **38**, 94–101. https://doi.org/10.1016/j.dnarep.2015.11.019 (2016).
66. Veigl, M. L. et al. Biallelic inactivation of hMLH1 by epigenetic gene silencing, a novel mechanism causing human MSI cancers. *Proc. Natl. Acad. Sci. U S A.* **95**(15), 8698–8702. https://doi.org/10.1073/pnas.95.15.8698 (1998).
67. Guo, R. J. et al. Microsatellite instability of papillary subtype of human gastric adenocarcinoma and hMLH1 promoter hypermethylation in the surrounding mucosa. *Pathol. Int.* **51**(4), 240–247. https://doi.org/10.1046/j.1440-1827.2001.01197.x (2001).
68. Choi, Y. Y. et al. Microsatellite instability and programmed cell death-ligand 1 expression in stage II/III gastric cancer: Post hoc analysis of the classic randomized controlled study. *Ann. Surg.* **270**(2), 309–316. https://doi.org/10.1097/SLA.0000000000002803 (2019).
69. Smyth, E. C. et al. Mismatch repair deficiency, microsatellite instability, and survival: An exploratory analysis of the medical research Council adjuvant gastric infusional chemotherapy (MAGIC) trial. *JAMA Oncol.* **3**(9), 1197–1203. https://doi.org/10.1001/jamaoncol.2016.6762 (2017).
70. Mizuguchi, A. et al. Genetic features of multicentric/multifocal intramucosal gastric carcinoma. *Int. J. Cancer* **143**(8), 1923–1934. https://doi.org/10.1002/ijc.31578 (2018).
71. Kim, D. G. et al. Clinical implications of microsatellite instability in early gastric cancer. *J. Gastric Cancer.* **19**(4), 427–437. https://doi.org/10.5230/jgc.2019.19.e38 (2019).

Acknowledgements

Author contributions

J.C. contributed to the acquisition of clinical samples, data collection and analysis. J.C. drafted the original manuscript. X.C. revised the manuscript. C.Z. designed the study. M.J. gave professional comments on the study and supervised the work. All authors contributed to the article and approved the submitted version.

Declarations

Competing interests

The authors declare no competing interests.

Additional information

Correspondence and requests for materials should be addressed to C.Z. or M.J.

Reprints and permissions information is available at www.nature.com/reprints.

Publisher's note Springer Nature remains neutral with regard to jurisdictional claims in published maps and institutional affiliations.